Pharm Res (2013) 30:2654–2663
DOI 10.1007/s11095-013-1091-7

RESEARCH PAPER

Micellar Delivery of Flutamide Via Milk Protein Nanovehicles Enhances its Anti-Tumor Efficacy in Androgen-Dependent Prostate Cancer Rat Model

Ahmed O. Elzoghby • Maged W. Helmy • Wael M. Samy • Nazik A. Elgindy

Received: 19 February 2013 / Accepted: 28 May 2013 / Published online: 6 June 2013

ABSTRACT

Purpose This article describes the preparation, physicochemical characterization and *in vivo* assessment of parenteral colloidal formulation of flutamide (FLT) based on biocompatible casein (CAS) self-assembled micelles in order to control drug release, enhance its antitumor efficacy and reduce its hepatotoxicity.

Methods Spray-drying technique was successfully utilized to obtain solidified redispersible drug-loaded micelles.

Results Spherical core-shell micelles were obtained with a particle size below 100 nm and a negative zeta potential above −30 mV exhibiting a sustained drug release up to 5 days. After intravenous administration into prostate cancer bearing rats for 28 days, FLT-loaded CAS micelles showed a higher antitumor efficacy as revealed by significantly higher reduction in PSA serum level (65.95%) compared to free FLT (55.43%). Moreover, micellar FLT demonstrated a marked decrease in relative weights of both prostate tumor and seminal vesicle (34.62 and 24.59%) compared to free FLT (11.86 and 17.74%), respectively. These antitumor responses were associated with notable reduction of cell proliferation, intratumoral angiogenesis and marked increase of tumor apoptosis. A significantly lower risk of hepatotoxicity was observed by micellar FLT as evidenced by lower alanine aminotransferase (ALT) serum level compared to free FLT.

Conclusions Overall this approach suggested that CAS micelles might be an ideal candidate for intravenous delivery of hydrophobic anticancer drugs.

A. O. Elzoghby (✉) · W. M. Samy · N. A. Elgindy
Department of Industrial Pharmacy, Faculty of Pharmacy
Alexandria University, Alexandria, Egypt
e-mail: dr_ahmedelzoghby@yahoo.com

M. W. Helmy
Department of Pharmacology and Toxicology, Faculty of Pharmacy
Pharos University, Alexandria, Egypt

W. M. Samy
Department of Pharmaceutics and Pharmaceutical Technology
Faculty of Pharmacy, Beirut Arab University, Beirut, Lebanon

KEY WORDS anti-tumor efficacy · casein micelles · hepatotoxicity · hydrophobic anti-cancer drugs · prostate cancer · spray-drying

INTRODUCTION

Prostate cancer (PCa) is one of the most common cancers all over the world. Statistically it has overtaken lung and colon cancers to be the most common cancer in male (1). By blocking the androgen receptor, anti-androgens e.g., flutamide (FLT) and bicalutamide represent an efficient alternative as monotherapy or combined to castration for locally advanced and metastatic androgen-dependent PCa (1). However, the clinical application of FLT is largely hampered by its low bioavailability attributed to its poor aqueous solubility and rapid first pass hepatic metabolism with a relatively short half-life of 5–6 h in addition to serious hepatotoxicity (2). Therefore, a novel drug delivery system (DDS) is required in order to solubilize and control the release rate of this poorly soluble anti-cancer drug.

Inclusion complexes (2,3), co-lyophilized dispersions (4,5), liquisolid compacts (6), liposomes (7), nanoemulsions (8), self-nanoemulsifying DDS (9) and polymeric microspheres (10) have been investigated to overcome the insolubility and provide controlled release of FLT. Polymers, oils or surfactants were used in these formulations to solubilize FLT. Although these non-endogenous materials are biodegradable, they may cause problems of slow clearance and immunogenicity when administered intravenously. Casein (CAS), the major milk protein, is much superior to these materials as a GRAS protein that forms an integral part of our daily diet (11). In aqueous solutions, CAS molecules have the ability to self-assemble into spherical micelles (*ca.* 50–500 nm in diameter) owing to their amphiphilic nature comprising hydrophobic and hydrophilic amino acid residues (12). In recent years, CAS micelles were recognized as potential delivery vehicles

for nutraceutical and pharmaceutical materials (13–17). Hydrophobic bioactives including vitamins (e.g., vitamin D_2 (13) and A (14)), polyphenols (e.g. curcumin (15)) and lipophilic drugs (e.g., mitoxantrone, paclitaxel (16) and celecoxib (17)) could be successfully incorporated into the hydrophobic core of CAS micelles, thus providing the potential for solubilization of poorly soluble drugs.

Different techniques can be applied to prepare drug-loaded polymeric micelles, including direct dissolution, dialysis, solution casting, emulsification and lyophilization (18,19). In our laboratory, spray-drying technique was successfully used for preparation of genipin-crosslinked CAS micelles for prolonged release of alfuzosin hydrochloride (20). The results demonstrated a sustained drug release with the % release could be monitored via modulating genipin-crosslinking density (20). More recently, cisplatin-loaded CAS nanoparticles have demonstrated prominent tumor targeting ability and superior anti-tumor efficacy after intravenous administration in hepatic tumor-bearing mice model compared to free cisplatin (21). These nanoparticles were prepared by polymerizing acrylic acid in the presence of CAS crosslinked with transglutaminase. However, this procedure has some drawbacks including the chemical initiator required by polymerization process and the residual monomers of the nonbiodegradable acrylic acid in addition to the high temperature used in the preparation process.

In our previous study, CAS micelles were able to enhance the solubilization and controlled delivery of FLT with a prolonged systemic circulation (22). In this study, a friendly spray-drying procedure was successfully utilized to develop redispersible solidified CAS micellar system for intravenous delivery of FLT, aiming at prolonging the drug release, improving its anti-tumor efficacy, and reducing the associated side effects. The physicochemical characteristics, morphology and *in vitro* drug release were investigated. More importantly, the *in vivo* anti-tumor, anti-proliferative, anti-angiogenic and apoptotic activity in addition to the associated hepatotoxicity of CAS-FLT micellar formulations were assessed in male rats bearing androgen-dependent PCa compared to free FLT after intravenous administration.

MATERIALS AND METHODS

Materials

Casein (CAS) from bovine milk, technical grade, nitroso methyl urea (NMU), cyproterone acetate and testosterone were purchased from Sigma-Aldrich (St. Louis, USA). Flutamide (FLT) was kindly donated by Archimica chemical company (Origgio, Italy). Polyoxyethylene sorbitan monooleate (Tween 80) was from (Riedel-de Häen, Germany). Sodium azide was obtained from LOBA Chemie Pvt., Ltd. (Mumbai, India). Poly(ethylene glycol) 200 (PEG-200) was supplied by Pharaonia Pharmaceuticals (Alexandria, Egypt). All other chemicals were of analytical grade and used without further purification.

Preparation of FLT-Loaded CAS Micelles

A calculated amount of FLT was dissolved in 95% ethanol and then added dropwise to a 10 mg/mL aqueous CAS solution (pH 7.4) under moderate magnetic stirring for 5 h. The micellar solution was then spray-dried using a Büchi B-290 Mini-Spray Dryer (Flawil, Switzerland), equipped with a high-performance cyclone, with a two-component nozzle and current flow, with inlet temperature of 150°C, outlet temperature of 90°C, aspiration air of 90%, feed flow of 5 mL/min, spraying pressure of 5.0–5.8 mbar, and air flow rate of 320 L/h. Unloaded CAS micelles (F_1) were prepared the same as above but without using drug. The spray-dried micelles were stored in a desiccator at 25°C till further analysis. The composition of spray-dried unloaded and FLT-loaded CAS micelles with various drug/protein mass ratios is illustrated in Table I.

Physicochemical Characterization of FLT-CAS Micelles

For drug content determination, an accurately weighed amount of the spray-dried micelles was digested in methanol under ultrasonication to dissolve FLT. This solution was then filtered through a 0.45 μm membrane filter, and the drug was determined by an HPLC method with the following conditions: Spheri-5, RP C18 column (220 mm× 4.6 mm, pore size 5 μm, Perkin Elmer, USA) and a UV detector, the mobile phase: methanol–water (75:25, v/v), flow rate: 1.0 mL/min, and measured wavelength: 304 nm (3–5). The percentage drug loading (%DL) and incorporation efficiency (%IE) for each formula were calculated as previously described (22).

The size and zeta potential of spray-dried FLT-loaded CAS micelles in aqueous solution was determined using a DLS analyzer (NanoZS/ZEN3600 Zeta Sizer, Malvern Instruments, UK) as previously described (20,22). The morphology of the micelles (F_3) was examined using a transmission electron microscope (TEM, JEOL 1200EX, JEOL Ltd., Japan) as previously described (20,22). To evaluate the drug release from CAS micelles, spray-dried FLT-loaded CAS micelles (equivalent to 20 mg drug) were suspended in PBS, pH 7.4, placed into a cellulose ester dialysis tube (cutoff 12–14 kDa) and dialyzed against 900 mL PBS (pH 7.4) containing 0.2% Tween 80 and 0.02% sodium azide as a preservative. The entire system was incubated at 37±0.5°C under stirring at 100 rpm. At predetermined time points, 5 mL of the release medium was removed and replaced with the same volume of

Table I Composition and Physicochemical Properties of Spray-Dried Unloaded and FLT-Loaded CAS Micelles (Values are the Mean ± S.D., $n=3$)

Formula	Variable	DL (% w/w)	IE (% w/w)	Particle size (nm)	Zeta potential (mV)
FLT/CAS mass ratio					
F_1	–	–	–	91.2 ± 5.04	−35.6 ± 4.48
F_2	1:8	9.49 ± 0.41	95.74 ± 3.96	93.24 ± 3.48	−33.6 ± 3.73
F_3	1:10	6.66 ± 0.26	96.18 ± 1.55	74.60 ± 2.56	−37.3 ± 4.47
F_4	1:15	4.77 ± 0.56	92.54 ± 2.80	62.43 ± 3.34	−34.7 ± 2.96

dissolution medium. In comparison, FLT was dissolved in a cosolvent mixture of 0.9% w/v NaCl/ethanol/PEG-200 (2:1:3 v/v/v) (F_0) (2). The amount of FLT released was determined by an HPLC method. Release kinetics were evaluated by fitting the obtained release data into first order, zero order and Higuchi equations (20).

Induction of Androgen-Dependent PCa in Rats

In vivo experiments were performed on male Sprague Dawely rats (200 ± 20 g) housed in stainless-steel mesh cages, under standard conditions of light illumination, relative humidity and temperature and had free access to standard laboratory food and water throughout the study. All procedures were performed according to a protocol approved by the Animal Care and Use Committee (ACUC) of Faculty of Pharmacy, Alexandria University and in accordance with regulations of the National Research Council's guide for the care and use of laboratory animals.

Androgen-dependent PCa was induced in the male rats at the age of 45 days, by daily intra-peritoneal injection of 50-mg/kg of cyproterone acetate for 3 weeks, followed by 3 days intramuscular injection of 100 mg/kg of testosterone. At the age of 70 days, all rats received a single intravenous injection of 50 mg/kg of the carcinogenic agent nitroso methyl urea (NMU) (23). Then, rats received testosterone (100 mg/kg) at the same day of NMU injection and every 7 days later on along days of experiment. Rats' prostate-specific antigen (PSA) serum level was determined at the day of NMU injection and every 15 days using RayBio® PSA-total ELISA Kit, Cat#: ELH-PSATOTAL-001 (RayBiotech, Inc., USA) according to the manufacturer's protocol. Similar to human-being, rats showing doubling or more of the basal PSA level are considered to be suspicious to develop PCa. This abnormal PSA level was confirmed with a repeat test. Prostate tissues of 7 rats showing elevated PSA level were isolated and histopathological analysis was performed for further confirmation of PCa development (24).

In Vivo Anti-Tumor Efficacy

After confirmation of PCa development, rats showing elevated PSA level were randomly assigned into three groups of eight rats each: the first group was treated with FLT-loaded CAS micellar formulation (F_3), the second group was treated with free FLT solution (F_0) in a cosolvent mixture of 0.9% w/v NaCl/ethanol/PEG-200 (2:1:3 v/v/v). Both groups were injected, under ether anesthesia, with FLT formulation (eq. to 12 mg FLT/kg) into the tail vein of rats twice per week for a treatment period of 28 days. A third positive control group of PCa-bearing rats receives only saline without FLT treatment. Parallel to the three groups, a negative control group of eight healthy male rats of the same age and body weight were kept under the same conditions as other groups.

PSA serum level was determined every 14 days during the treatment period. Blood samples were collected and the serum was separated by allowing blood to clot for 30 min at room temperature before centrifugation at 5,000 rpm for 20 min. Serum was assayed for PSA level in freshly separated samples (24). At the end of treatment period, animals were sacrificed by cervical dislocation. Prostate and seminal vesicle wet weights were determined. Each excised dorsolateral lobe of the prostate was divided into 2 equal parts. The first part was fixed in 10% neutral buffered formalin and embedded in paraffin blocks for histopathological examination. The second part was homogenized using PBS and aliquots were preserved at −80°C for further determination of markers of anti-tumor activity.

Histopathological Analysis

3–5 mm prostate tissue sections were cut, deparaffinized, rehydrated, and stained with hematoxylin and eosin (H&E). Thereafter stained tissue sections were dehydrated, mounted in DPX (Fluka Chemie GmbH, Buchs, Germany) and digital images were produced using Olympus AX70 light microscope with a digital camera (Sweden) for histopathological changes in rat prostate tissue.

Immunohistochemical Analysis

Analysis of the effect of free FLT (F_0) and FLT-loaded CAS micellar formulation (F_3) on proliferation of PCa cells in rats was performed using Ki-67 antibody. Tissue specimens were processed for immunohistochemical analysis as described previously (25). Neutral buffered formalin-fixed tissue was embedded in paraffin. Tissue sections (5 mm) were prepared using a

microtome and mounted on slides. Immunohistochemical analysis was done within 24 h of the sections being cut. Sections were deparaffinized in xylene, rehydrated in graded alcohols (100, 95 and 75% v/v) and washed in distilled water. Endogenous peroxidase activity was quenched with 0.01% H_2O_2. Further, sections were treated with 0.05% trypsin, 0.05% $CaCl_2$ in Tris–HCl (pH 7.6) for 5 min at 37°C. Antigen retrieval was done by microwaving the sections in 10 mM/L citric acid (pH 6.0) for 30 min. The slides were washed thrice in PBS and blocked with 10% normal horse serum for 30 min. Tissue sections were then incubated with prediluted (1:50) rabbit monoclonal antibody Ki-67 clone SP6 (Dako, Glostrup, Denmark) for 3 h at 4°C. After being washed thrice with PBS, the sections were incubated with biotinylated anti-mouse immunoglobulins (1:500) for 30 min at room temperature. The slides were then washed thrice in PBS, labeled using avidin-biotin peroxidase complexes (1:25) for 30 min at room temperature and then washed with PBS. Immunoreactivity was determined using diaminobenzidine (DAB) as the final chromogen. Finally, sections were counterstained with Meyer's hematoxylin, dehydrated through a sequence of increasing concentrations of alcohol, cleared in xylene and mounted with epoxidic medium. The immunohistochemical signals of Ki-67 were further quantified by the use of digital image analysis technique (26). The Image J software (version 1.45 s) together with computer-assisted microscopy was employed for this purpose.

Detection of Angiogenesis and Apoptosis

Quantification of microvessel formation (angiogenesis) was determined by measuring the levels of the angiogenic factors; vascular endothelial growth factor (VEGF) and Insulin-like growth factor-1 (IGF-1) in tumor tissue homogenate using RayBio® VEGF ELISA Kit, Cat#: ELR-VEGF-001 and RayBio® IGF ELISA Kit, Cat#: ELH-IGFI-001, respectively (RayBiotech, Inc., USA) according to the manufacturer's protocol. Results were quantified by reading the optical density at 450 nm. Quantitative determination of Caspase-3 level in tumor tissue homogenate as a marker of tumor apoptosis induction was performed using Caspase-3 instant ELISA kit™, Cat#: BMS2012INST (Bender MedSystems GmbH, Vienna, Austria) by following the manufacturer's instructions. Results were quantified by reading the absorbance at 450 nm.

Estimation of Hepatotoxicity

Liver damage was examined through the measurement of Alanine aminotransferase (ALT) level in rat serum. After the animals were treated with the free drug (F_0) or micellar formulation (F_3) for 28 days, 1 mL of blood from each rat was collected, serum was separated by centrifugation at 5,000 rpm for 20 min and ALT level was measured using ALT-Colorimetric standard diagnostic kit (Spectrum Diagnostics, USA).

Statistical Analysis

Statistical comparisons between treated groups were analyzed using one-way analysis of variance (ANOVA) followed by Newman–Keuls multiple comparison test. A significant difference between treatments was concluded when $P<0.05$ using Graph pad prism, version 3.02.

RESULTS AND DISCUSSION

Physicochemical Properties of the Micelles

Caseins are amphiphilic proteins with high levels of hydrophobic and hydrophilic amino acid residues. Therefore, caseins exhibit a strong tendency to self-assemble into spherical CAS micelles (11,12). Previously, we have reported the preparation of a CAS micellar formulation of FLT via spray-drying technique (22). In the present study, we sought to investigate the feasibility of using the spray-dried FLT-loaded CAS micelles for treatment of androgen-dependent PCa in rats. Our data showed that FLT can be incorporated in the micelles with a good incorporation efficiency (92.54 to 96.18%) and drug loading (4.77 to 9.49%) (Table I). Successful FLT binding to CAS micelles may be attributable to strong hydrophobic interactions between the poorly soluble drug with the hydrophobic core of protein micelles (16,22).

The size of the spray-dried FLT-loaded CAS micelles as measured by DLS revealed that the mean diameter of the micelles was in the range of 62.43–93.24 nm with a parallel increase in the micellar size was observed upon increasing the drug loading from 1:15 to 1:8 FLT-CAS mass ratio (Table I) (27). The micelles were negatively charged with a zeta potential value of −33.6 to −37.3 mV revealing a good colloidal stability. This is corresponding to the negative surface charge on CAS molecules above its isoelectric point, 4.6 (16,22) (Table I). Figure 1a shows representative TEM micrograph of FLT-loaded CAS micelles (F_3) where most of the micelles had a spherical shape with a well-defined core-shell structure. These findings are in agreement with the characteristic core–shell nanoassembly of CAS micelles owing to its amphiphilic nature where a hydrophobic core is surrounded by a hydrophilic "hairy" corona of κ-CAS (11,28).

The release of FLT from the spray-dried CAS micellar formulations was slow. It took 5 days for about 95.57, 88.65, and 74.88% of FLT to be released from micelles prepared with 1:8, 1:10, and 1:15 drug-protein ratio, respectively. The

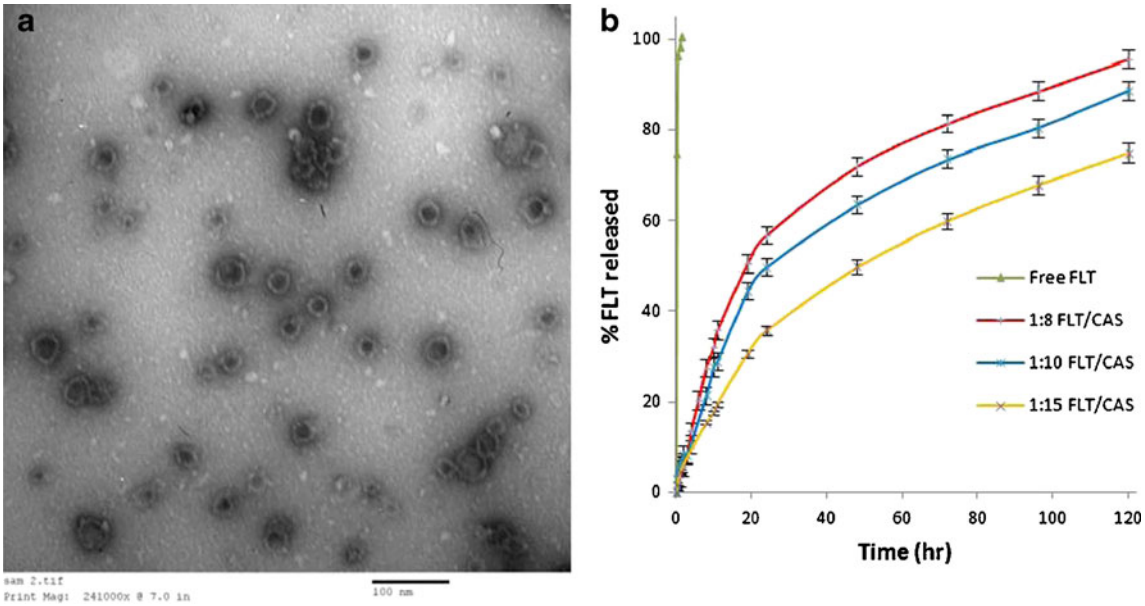

Fig. 1 *In vitro* characteristics of FLT-loaded CAS micelles: (**a**) Transmission electron micrograph of FLT-loaded CAS micelles (F_3) and (**b**) *In vitro* FLT release from CAS micelles prepared with various drug/protein mass ratios in PBS (pH 7.4) at 37°C compared to free FLT.

diffusion of the free FLT out of the dialysis tube was much faster with >80% of free FLT was rapidly released within the first 2 h (Fig. 1b). This result showed that the micelle carrier cannot only solubilize the poorly soluble drug, FLT, but also sustain its release. Slow drug release from polymeric micelles i.e. depot effect, allows for accumulation of polymeric micelles at target sites with minimal drug loss and localized drug release (18). The mechanism of drug release from CAS micelles would be non-Fickian type of drug diffusion according to the n values ($0.45 < n < 0.89$) calculated by the Korsmeyer–Peppas model, as shown in Table II, indicating that the release of FLT from CAS micelles may be controlled by coupled diffusion/polymer relaxation. This result is in accordance with earlier findings (20).

In Vivo Antitumor Efficacy

There is a substantial interest in developing therapeutic options for treatment of prostate cancer based on use of nanodevices, to overcome the lack of specificity of conventional chemotherapeutic agents as well as for the early detection of precancerous and malignant lesions. In our previous study (22), genipin-crosslinked FLT-CAS micelles exhibited more prolonged circulation and sustained drug release than uncrosslinked ones. However, in the present study, we selected the uncrosslinked FLT-loaded CAS micelles for *in vivo* treatment of prostate cancer-bearing rats because the uncrosslinked micelles have succeeded to retard the drug release *in vitro* (up to 5 days) and *in vivo* with no remarkable difference from crosslinked micelles in addition to the relatively higher drug content, smaller size and better aqueous redispersility of the uncrosslinked micelles (22). In our work, *in vivo* animal studies were carried out to examine the anti-tumor effect of FLT-loaded CAS micelles compared to free drug using an androgen-dependent PCa rat model successfully induced using the reported (NMU+ Testosterone) method (23). In PCa, prostate-specific antigen (PSA) has turned out to be a very important marker. This antigen is elevated in the serum in virtually all patients who have advanced hormone-dependent disease. The transcription of PSA is a hormone dependent process; the PSA promoter contains two androgen-responsive elements (29). Therefore, PCa development was confirmed in our study by rats showing doubling or more than double value of the basal PSA level. Preliminary experiments showed no significant effect for each of the cosolvent alone or the unloaded CAS micelles (F_1) on PCa progression in rats.

Figure 2a shows the progress of PSA serum level observed in rats treated with free FLT (F_0) and FLT-CAS micelles (F_3) for 14 and 28 days in addition to the negative control healthy rats and positive control PCa bearing rats that have not received any further treatment. Treatment of rats with free FLT (F_0) at a dose of 12 mg/kg body weight for 14 and 28 days resulted in 12.84 and 55.43% reduction in PSA level, respectively. In comparison, at the same dose, spray-dried FLT-loaded CAS micelles (F_3) caused a significantly higher % reduction in PSA level (42.45 and 65.95%) after 14 and 28 days, respectively ($P<0.05$ and $P<0.01$ after 14 and 28 days, respectively). Besides PSA level measurement, the % relative weights of prostate and seminal vesicle to the rat body weight for the positive control rats were compared with those of FLT-treated rats at the end of the 28 day treatment period. Administration of free FLT (F_0) decreased the relative

Table II Release Kinetic Parameters of FLT-Loaded CAS Nanoparticles in PBS (pH 7.4) at 37°C

Formula	FLT/CAS mass ratio	Zero order	First order	Higuchi	Korsmeyer-Peppas	
		R^2	R^2	R^2	R^2	*n*
F_2	1:8	0.838136	0.976676	0.978008	0.896996	0.71044
F_3	1:10	0.874692	0.982707	0.984018	0.936384	0.54624
F_4	1:15	0.915331	0.98489	0.993936	0.979746	0.69007

prostate and seminal vesicle weights by 11.86 and 17.74%, respectively. At the same dose, micellar FLT (F_3) generated a significantly higher % reduction in the relative prostate and seminal vesicle weights (34.62 and 24.59%), respectively ($P<0.001$ for prostate and $P<0.05$ for seminal vesicle) compared to free drug (Fig. 2b).

The significantly higher % reduction in PSA serum level and relative weights of prostate and seminal vesicle caused by FLT-CAS micelles compared to free FLT could be attributed to the "enhanced permeation and retention" (EPR) effect of the nano-sized FLT delivery system. FLT-CAS micelles (F_3) having a size of 74.6 nm are likely to freely pass through the leaky endothelial junctions of the capillaries in tumor tissue, but not in normal tissue (30). Similarly, polymeric micellar formulations of the anti-androgen, bicalutamide, composed of poly(ethylene glycol)-b-poly(L-lactide) and methoxypoly(ethylene glycol)-b-poly(carbonate-co-L-lactide) enhanced its antitumor activity as demonstrated by their significant inhibition of tumor growth in PCa xenograft-bearing mice and LNCaP human PCa cell lines, respectively (31,32). Prostate tumor growth was effectively regressed upon treatment with bicalutamide up to 20 days post-treatment. Formulation into poly(ethylene glycol)-b-poly(L-lactide) micelles more significantly regressed tumor growth (31).

Histopathological and Immunohistochemical Analysis

Histopathological studies of haematoxylin and eosin (H&E) stained sections of the isolated prostate samples from different treated rat groups are summarized in Fig. 3H&E. In the sections of normal dorsolateral prostate (DLP) of negative control group, the tubules were lined by a single layer of cuboidal cells with secretions in the lumen (Fig. 3H&E, a). In the positive control group of rats, a large number of hyperplasic and dysplasic lesions were observed indicating the induction of PCa (Fig. 3H&E, b). The vast majority of lesions were adenoma and adenocarcinoma. The tubules were of varying sizes and contain regions composed of more than one layer of epithelial cells. Moreover, numerous papillary projections were present. These induced pathological changes closely mimic the histological features found in human prostatic dysplasia (23). In our present investigation,

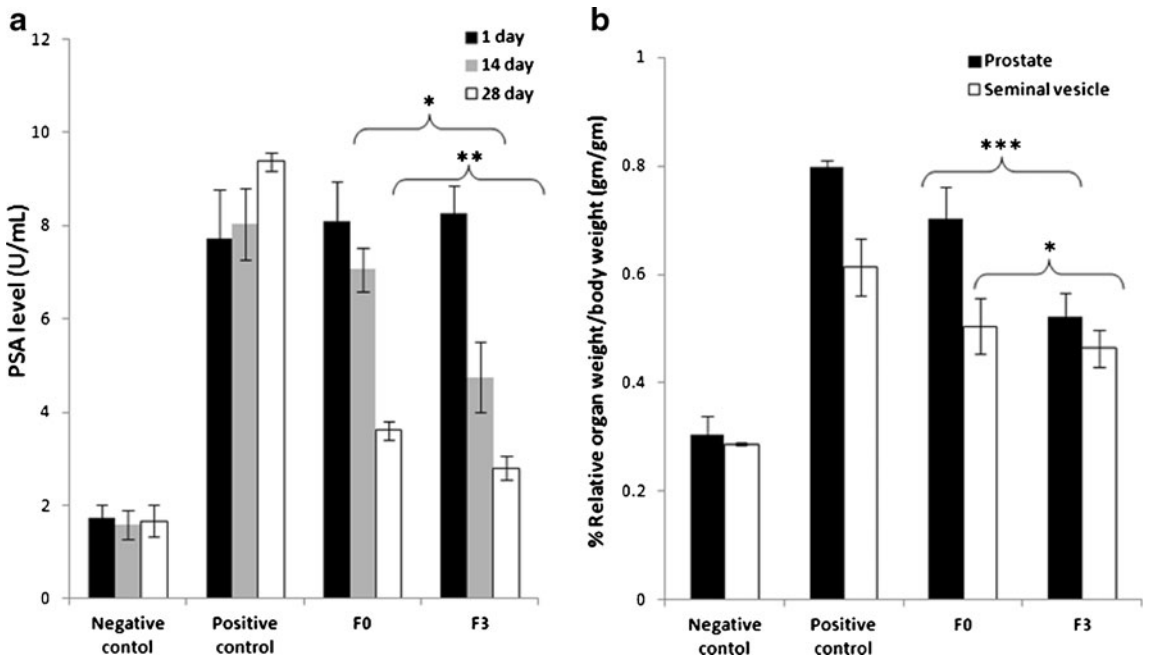

Fig. 2 *In vivo* anti-tumor efficacy of FLT formulations: (**a**) Changes in prostate specific antigen (PSA) serum level and (**b**) Changes in % relative weight of prostate and seminal vesicle to rat body weight in negative control, positive control and rats treated with free FLT (F_0) and FLT-loaded CAS micelles (F_3) after i.v. administration at a dose of 12 mg/kg. Statistical differences between the two treatment groups F_0 and F_3 $^*P<0.05$, $^{**}P<0.01$, $^{***}P<0.001$.

treatment of rats with either free FLT (F_0) or FLT-loaded CAS micelles (F_3) at a dose of 12 mg/kg for 28 days succeeded to significantly reduce the hyperplasic and dysplasic lesions in the dorsolateral lobes of prostate compared to positive control animals (Fig. 3H&E, c and d). These findings ensure that any of the two preparations succeeded to release FLT in such a manner that achieves the therapeutic goals.

To investigate potential mechanisms underlying the efficacy of micellar FLT-based therapy *in vivo*, we examined its effects on tumor cell proliferation using Ki-67 staining. Ki-67 is a nuclear protein associated with somatic cell proliferation and so considered as a direct marker of proliferation of cancer cells. Ki-67 was suggested as a useful biomarker to predict PCa progression with patients after endocrine treatment (33). The images observed by microscopy revealed that Ki-67 was strongly stained in the positive control tumor compared to the negative control one (Fig. 3Ki-67, a and b). In contrast, the density of staining from rat tumor treated with free FLT (F_0) was decreased reflecting a reduced number of Ki-67 stained cells (Fig. 3Ki-67, c). Especially, the density of staining from rat tumor treated with FLT-CAS micelles (F_3) was much weaker than that from the other groups (Fig. 3Ki-67, d). These results suggest that FLT-loaded CAS micelles exhibit a particularly high potency in the inhibition of cellular proliferation thereby suppressing the tumor growth. Similarly, formulation of docetaxel into poly(lactide-co-caprolactone) and poly(lactide-co-caprolactone-co-glycolide) nanoparticles proved an increased antiproliferative efficacy against PCa cells compared with free drug (34).

Moreover, digital image analysis technique was used for quantification of the % expression of the proliferative marker Ki-67 in rat prostate tissues (Fig. 4) (26). Results showed that Ki-67 was highly expressed (69.29%) in adenomas of the positive control compared to negative control rats (39.70%) ($P<0.001$). A marked reduction of Ki-67 expression was noted in micellar FLT (F_3)-treated group (33.58%) after administration for 28 days at a dose of 12 mg/kg compared with free FLT (F_0)-treated group (20.2%) ($P<0.001$, Fig. 4). Thus, FLT-loaded CAS micelles generated a more significant decrease of the tumor proliferative activity than did free FLT.

Angiogenesis and Apoptosis

Angiogenesis is a critical element of solid tumor growth and metastasis; therefore, PCa requires new vasculature to continue its uncontrolled growth. Angiogenesis-stimulating factors including vascular endothelial growth factor (VEGF) and insulin-like growth factor-1 (IGF-1) are increased in PCa (35–37). VEGF is one of the most crucial mediators of tumor angiogenesis and is closely involved in tumor development and metastasis. IGF-1 has mitogenic, angiogenic and anti-apoptotic effects on both normal and transformed prostate epithelial cells *in vitro* and *in vivo* (35–37).

To test the anti-angiogenic potency of FLT-loaded CAS micelles (F_3) and free FLT (F_0), we studied the expression of VEGF and IGF-1 proteins in the PCa tissue of rats treated with the two FLT formulations in addition to the negative and positive control rats. As shown in Fig. 5a, overexpression of VEGF and IGF-1 proteins has been demonstrated in PCa tissue of positive control rats. The up-regulations of VEGF and IGF-1 proteins expression were suppressed by treatment with both FLT formulations. Both free FLT (F_0) and FLT-loaded CAS micelles (F_3) significantly reduced the level of both angiogenic growth factors; VEGF by 35.71 and 36.97%, respectively, and IGF-1 by 38.51 and 45.24%, respectively, compared to the untreated positive control rats ($P<0.01$ for both VEGF and IGF-1). However, no significant difference was observed between the two FLT treatment groups F_0 and F_3 ($P>0.05$ for both VEGF and IGF-1).

Androgen receptor is essential for prostate normal and cancer cell growth. Apoptosis is lagged behind androgen receptor down-regulation and caspases activation, and is the accumulative effect (38). Because caspases are the molecular instigators of apoptosis, we measured the level of caspase-3 in the PCa tissue of rats to detect apoptosis of tumor cells within tumor tissue (39). As shown in Fig. 5b, significant increases of caspase-3 activation were found in both free (F_0) and micellar FLT (F_3)-treated groups compared with the untreated positive control rats ($P<0.05$). Free FLT and FLT-loaded CAS micelles caused 64.77 and 66.29% elevation in caspase-3 level,

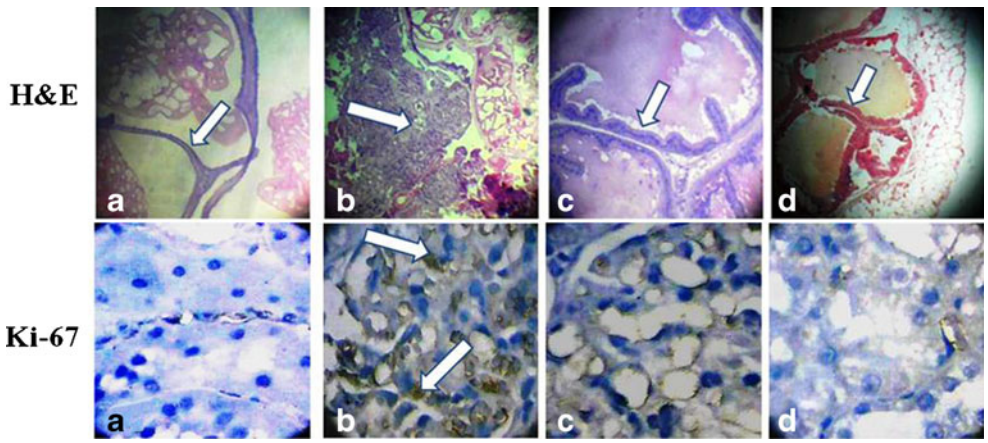

Fig. 3 (H&E) Histopathological appearance (Magnification × 100) and (Ki-67) Immunohistochemical staining of Ki-67 (Magnification × 400) of dorsolateral prostate (DLP) sections dissected from different tested rat groups; (**a**) Negative control rats, (**b**) Positive control rats, and rats treated with: (**c**) Free FLT (F_0) or (**d**) FLT-loaded CAS micelles (F_3) at a dose of 12 mg/kg for 28 days.

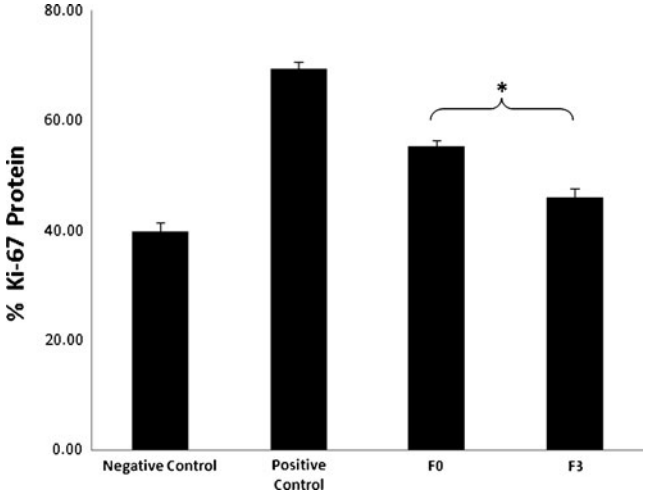

Fig. 4 % Expression of the proliferation marker (Ki-67), calculated by digital image analysis technique, in rat prostate tissues of the negative control, positive control and rats treated with free FLT (F_0), and FLT-loaded CAS micelles (F_3) at a dose of 12 mg/kg for 28 days. Statistical differences between the two treatment groups F_0 and F_3 $^*P < 0.001$.

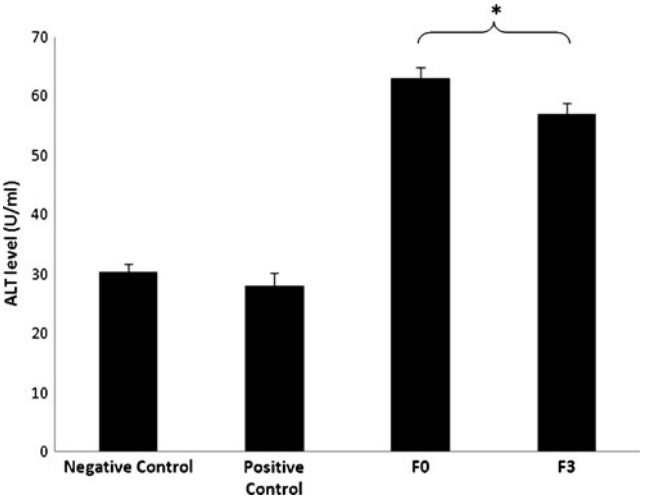

Fig. 6 Alanine aminotransferase (ALT) serum level in the negative control, positive control and rats treated with free FLT (F_0), and FLT-loaded CAS micelles (F_3) at a dose of 12 mg/kg for 28 days. Statistical differences between the two treatment groups F_0 and F_3 $^*P < 0.05$.

respectively with no significant difference between them ($P > 0.05$). These results suggested that the administration of FLT-CAS micelles could effectively trigger tumor cell apoptosis *in vivo* compared to untreated positive control rats. Thus, it may be hypothesized that the antitumoral effects of FLT-CAS micelles could be attributed to its ability to reduce tumor cellular proliferation, inhibit intratumoral angiogenesis and increase promotion of tumor apoptosis.

Alanine Aminotransferase (ALT) Estimation

Since hepatotoxicity is the main limitation of therapeutic potential of FLT. In this study, we estimated the ALT serum levels in rats to monitor the reported hepatotoxicity of FLT. From Fig. 6, it is evident that ALT level in rats treated with free drug, F_0 (63 U/mL) was significantly higher than that treated with spray-dried FLT-loaded CAS micelles (F_3) (57

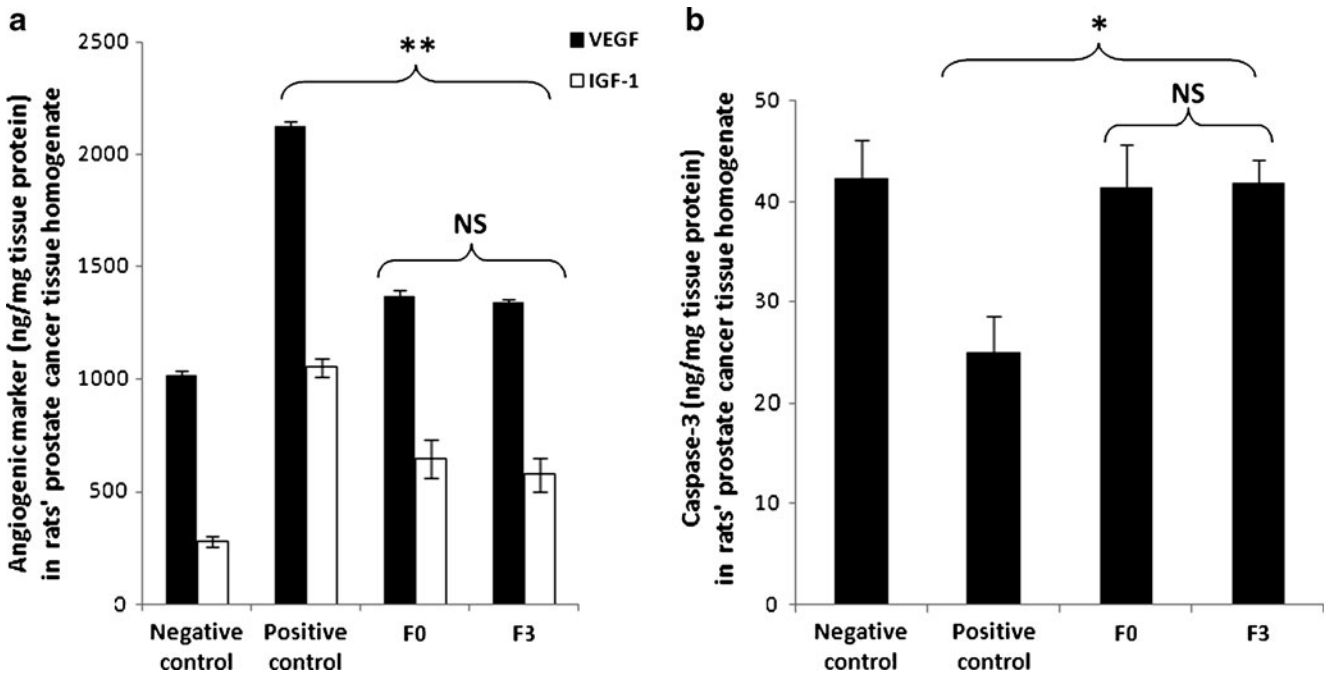

Fig. 5 (**a**) Angiogenesis of rat prostate cancer cells expressed as angiogenic marker (VEGF and IGF-1) level, and (**b**) Apoptosis of rat prostate cancer cells expressed as caspase-3 activity in prostate tissue homogenate from negative control, positive control and rats treated with free FLT (F_0), and FLT-loaded CAS micelles (F_3) at a dose of 12 mg/kg for 28 days. Statistical differences between the two FLT-treated groups (F_0 and F_3) and the untreated positive control group $^*P < 0.05$, $^{**}P < 0.01$. NS: No significant differences between the two treatment groups F_0 and F_3 ($P > 0.05$).

U/mL), $P<0.05$. The increase of enzyme activity is related to the intensity of cellular damage. Therefore, increase of ALT activity may be the consequence of FLT-induced pathological changes of the liver. These results showed that micellar FLT may help in reduction of the undesired side effects associated with liver following free drug administration.

In our previous study (22), CAS micelles exhibited a prolonged plasma circulation of FLT after i.v. administration into rats compared to free drug. In this study, the increased half-life of micellar FLT was translated to marked improvements in antitumor activity and tolerability. It has been previously observed that polymeric nanocarriers below 100 nm effectively evade clearance mechanisms, resulting in prolonged plasma circulation, efficiently extravasate through the leaky tumor vasculature combined with impaired lymphatic drainage in tumor tissues resulting in a high interstitial concentration of drug-loaded nanocarriers retained in the tumor followed by non-specific or specific receptor-mediated internalization of drug-loaded nanocarriers (40). Therefore, it can be seen that the significantly higher antitumor activity caused by FLT-CAS micelles (74.6 nm) compared with free FLT could be attributed to both the prolonged plasma circulation and the "enhanced permeation and retention" (EPR) effect of FLT-CAS micelles.

CONCLUSIONS

In this study, micelles composed of the natural milk protein, casein (CAS), loaded with the poorly soluble anti-cancer drug, flutamide (FLT), were successfully developed. Solidification of FLT-loaded CAS micelles was carried out via spray-drying technique. FLT release was sustained as a result of encapsulation into the inner hydrophobic core of the micelles. *In vivo* assessment of FLT-CAS micelles revealed that the anti-tumor activity was higher for micellar FLT than free drug represented by the decrease in prostatic specific antigen (PSA) serum level, prostate and seminal vesicle relative weights in addition to the histopathological changes. Moreover, FLT-CAS micelles were found to efficiently reduce cellular proliferation of prostate tumor, inhibit tumor angiogenesis, and enhance tumor apoptosis induction. The risk of hepatotoxicity was also lower for drug micelles than for free drug. Given its promising anti-tumor effect and lower hepatotoxicity, FLT-CAS micelles could serve as a potentially novel therapeutic agent in the treatment of prostate tumors.

ACKNOWLEDGMENTS AND DISCLOSURES

The authors thank Archimica Chemical Company, Italy, for kind donation of FLT used in this study.

REFERENCES

1. Wirth MP, Hakenberg OW, Froehner M. Antiandrogens in the treatment of prostate cancer. Eur Urol. 2007;51:306–14.
2. Zuo Z, Tam YK, Diakur J, Wiebe LI. Hydroxypropyl-β-cyclodextrin flutamide inclusion complex. ii. Oral and intravenous pharmacokinetics of flutamide in rat. J Pharm Pharmaceut Sci. 2002;5:292–8.
3. Elgindy N, Elkhodairy K, Molokhia A, Elzoghby A. Lyophilization monophase solution technique for improvement of the physicochemical properties of an anticancer drug, flutamide. Eur J Pharm Biopharm. 2010;74:397–405.
4. Elgindy N, Elkhodairy K, Molokhia A, Elzoghby A. Lyophilization monophase solution technique for preparation of amorphous flutamide dispersions. Drug Dev Ind Pharm. 2011;37:754–64.
5. Elgindy N, Elkhodairy K, Molokhia A, Elzoghby A. Lyophilized flutamide dispersions with polyols and amino acids: preparation and in vitro evaluation. Drug Dev Ind Pharm. 2011;37:446–55.
6. Elkhodairy K, Samy W. Optimization and evaluation of micromeritic and release properties of high dose flutamide liquisolid systems. Lett Drug Des Discov. 2012;9:336–44.
7. Murthy RSR, Umrethia ML. Optimization of formulation parameters for the preparation of flutamide liposomes by 3(3) factorial 26-term logit model. Pharm Dev Technol. 2004;9:369–77.
8. Madhusudhan B, Rambhau D, Apte SS, Gopinath D. Oral bioavailability of flutamide from 1-o-alkylglycerol stabilized o/w nanoemulsions. J Disp Sci Technol. 2007;28:1254–61.
9. Jeevana JB, Sreelakshmi K. Design and evaluation of self-nanoemulsifying drug delivery system of flutamide. J Young Pharm. 2011;3:4–8.
10. Elgindy N, Elkhodairy K, Molokhia A, Elzoghby A. Biopolymeric microparticles combined with lyophilized monophase dispersions for controlled Flutamide release. Int J Pharm. 2011;411:113–20.
11. Elzoghby AO, Abo El-Fotoh WS, Elgindy NA. Casein-based formulations as promising controlled release drug delivery systems. J Control Release. 2011;153:206–16.
12. Elzoghby AO, Samy WM, Elgindy NA. Protein-based nanocarriers as promising drug and gene delivery systems. J Control Release. 2012;161:38–49.
13. Semo E, Kesselman E, Danino D, Livney YD. Casein micelle as a natural nanocapsular vehicle for nutraceuticals. Food Hydrocoll. 2007;21:936–42.
14. Bourassa P, N'soukpoe-Kossi CN, Tajmir-Riahi HA. Binding of vitamin A with Milk α- and β-caseins. Food Chem. 2013;138:444–53.
15. Esmaili M, Ghaffari SM, Moosavi-Movahedi Z, Atri MS, Sharifizadeh A, Farhadi M, et al. Beta casein–micelle as a nano vehicle for solubility enhancement of curcumin; food industry application. LWT-Food Sci Technol. 2011;44:2166–72.
16. Shapira A, Assaraf YG, Epstein D, Livney YD. Beta-casein nanoparticles as an oral delivery system for chemotherapeutic drugs: impact of drug structure and properties on co-assembly. Pharm Res. 2010;27:2175–86.
17. Bachar M, Mandelbaum A, Portnaya I, Perlstein H, Even-Chen S, Barenholz Y, et al. Development and characterization of a novel drug nanocarrier for oral delivery, based on self-assembled β-casein micelles. J Control Release. 2012;160:164–71.
18. Dufresne MH, Fournier E, Jones MC, Ranger M, Leroux JC. Block copolymer micelles—Engineering versatile carriers for drugs and biomacromolecules. In: Gurny R, editors. Saint-Priest: B.T. Gattefossé; 2003;96:87–102.
19. Le Garrec D, Gori S, Luo L, Lessard D, Smith DC, Yessine MA, et al. Poly(N-vinylpyrrolidone)-block-poly(D, L-lactide) as a new polymeric solubilizer for hydrophobic anticancer drugs: in vitro and in vivo evaluation. J Control Release. 2004;99:83–101.

20. Elzoghby AO, Samy WM, Elgindy NA. Novel spray-dried genipin-crosslinked casein nanoparticles for prolonged release of alfuzosin hydrochloride. Pharm Res. 2013;30:512–22.
21. Zhen X, Wang X, Xie C, Wu W, Jiang X. Cellular uptake, antitumor response and tumor penetration of cisplatin-loaded milk protein nanoparticles. Biomaterials. 2013;34:1372–82.
22. Elzoghby AO, Helmy MW, Samy WM, Elgindy NA. Elgindy spray-dried casein-based micelles as a vehicle for solubilization and controlled delivery of flutamide: formulation, characterization, and in vivo pharmacokinetics. Eur J Pharm Biopharm. 2013. doi:10.1016/j.ejpb.2013.01.005.
23. Bosland MC, Prinsen MK. Induction of dorsolateral prostate adenocarcinomas and other accessory sex gland lesions in male wistar rats by a single administration of N-Methyl-N-Nitrosourea, 7,12-Dimethylbenz(α)Anthracene, and 3,2-Dimethyl-4-Aminobiphenyl after sequential treatment with cyproterone acetate and testosterone propionate. Cancer Res. 1990;50:691–9.
24. Stephan C, Jung K, Lein M, Sinha P, Schnorr D, Loening SA. Molecular forms of prostate-specific antigen and human kallikrein 2 as promising tools for early diagnosis of prostate cancer. Cancer Epidemiol Biomark Prev. 2000;9:1133–47.
25. Dash R, Dmitriev I, Su ZZ, Bhutia SK, Azab B, Vozhilla N, et al. Enhanced delivery of Mda-7/IL-24 using a serotype chimeric adenovirus (Ad.5/3) improves therapeutic efficacy in low car prostate cancer cells. Cancer Gene Ther. 2010;17:447–56.
26. Kaczmarek E, Górna A, Majewski P. Techniques of image analysis for quantitative immunohistochemistry. Rocz Akad Med Bialymst. 2004;49:155–8.
27. Kadama Y, Yerramillia U, Bahadur A. Solubilization of poorly water-soluble drug carbamezapine in pluronic micelles: effect of molecular characteristics, temperature and added salt on the solubilizing capacity. Colloids Surf B Biointerfaces. 2009;72:141–7.
28. De Kruif CG, Zhulina EB. κ-Casein as a polyelectrolyte brush on the surface of casein micelles. Colloids Surf A. 1996;117:151–9.
29. Fritz HS, Ries K, Nik B, Wim CJH, Albert K, Mercedes L. Prostate-specific antigen: a surrogate endpoint for screening new agents against prostate cancer? Prostate. 2000;42:107–15.
30. Danquah MK, Zhang XA, Mahato RI. Extravasation of polymeric nanomedicines across tumor vasculature. Adv Drug Deliv Rev. 2011;63:623–39.
31. Danquah M, Li F, Duke III CB, Miller DD, Mahato RI. Micellar delivery of bicalutamide and embelin for treating prostate cancer. Pharm Res. 2009;26:2081–92.
32. Danquah M, Fujiwara T, Mahato RI. Self-assembling methoxypoly(ethylene glycol)-b-poly(carbonate-co-L-lactide) block copolymers for drug delivery. Biomaterials. 2010;31:2358–70.
33. Rubio J, Ramos D, López-Guerrero JA, Iborra I, Collado A, Solsona E, et al. Immunohistochemical expression of Ki-67 antigen, Cox-2 and Bax/Bcl-2 in prostate cancer; prognostic value in biopsies and radical prostatectomy specimens. Eur Urol. 2005; 48:745–51.
34. Sanna V, Roggio AM, Posadino AM. Novel docetaxel-loaded nanoparticles based on poly(lactide-co-caprolactone) and poly(lactide-co-glycolide-co-caprolactone) for prostate cancer treatment: formulation, characterization, and cytotoxicity studies. Nanoscale Res Lett. 2011;6:260.
35. Longoria RL, Cox MC, Figg WD. Antiangiogenesis: a possible treatment option for prostate cancer? Clin Genitourin Cancer. 2005;4:197–202.
36. Moul JW, Merseburger AS, Srivastava S. Molecular markers in prostate cancer: the role in preoperative staging. Clin Prostate Cancer. 2002;1:42–50.
37. Ma Y, Cheng Q, Ren Z, Xu L, Zhao Y, Sun J, et al. Induction of IGF-1R expression by EGR-1 facilitates the growth of prostate cancer cells. Cancer Lett. 2012;317:150–6.
38. Bustos-Obregón E, Esponda P. Increase in apoptosis and of the stress protein HSP70 in the mouse epididymis produced by the antiandrogen flutamide. Int J Morphol. 2009;27:463–8.
39. Budihardjo L, Oliver H, Lutter M, Luo X, Wang X. Biochemical pathways of caspase activation during apoptosis. Annu Rev Cell Dev Biol. 1999;15:269–90.
40. Gong J, Chen M, Zheng Y, Wang S, Wang Y. Polymeric micelles drug delivery system in oncology. J Control Release. 2012;159:312–23.